Effect of graphene oxide on mechanical properties and durability of cement mortar

Lounis Djenaoucine , Álvaro Picazo , Miguel A. Rubia , Amparo Moragues , Jaime C. Gálvez *

Posted Date: 31 July 2023

doi: 10.20944/preprints202307.2114.v1

Keywords: Graphene oxide; Cement; Mechanical properties; Durability.

Article

Effect of Graphene Oxide on Mechanical Properties and Durability of Cement Mortar

Lounis Djenaoucine [1], Álvaro Picazo [2], Miguel Ángel de la Rubia [1], Amparo Moragues [1] and Jaime C. Gálvez [1,*]

[1] Departamento de Ingeniería Civil: Construcción, E.T.S.I. Caminos, Canales y Puertos, Universidad Politécnica de Madrid, C/ Profesor Aranguren 3, 28040 Madrid, Spain; Lounis.djenaoucine@alumnos.upm.es, miguelangel.rubia@upm.es, amparo.moragues@upm.es and jaime.galvez@upm.es

[2] Departamento de Tecnología de la Edificación, E.T.S. de Edificación, Universidad Politécnica de Madrid, Avda. Juan de Herrera, 6, 28040 Madrid, Spain; a.picazo@upm.es

* Correspondence: jaime.galvez@upm.es; Tel.: +34-91-0674-125

Abstract: The effect of graphene oxide (GO) on mechanical strengths and durability of cement composites has been studied by preparing GO-modified cement mortars. Thermogravimetric analysis (TGA) and nuclear magnetic resonance (^{29}Si MAS-NMR) were performed on the cement paste to research the influence of GO on the hydration process and chain structure of calcium-silicate-hydrate (C-S-H) gels. In addition, mechanical strength test, such as compressive and flexural, were performed on cement mortars. The addition of GO at 0.05 wt.% (by weight of cement) increased the compressive strength by 9.02% after 28 days. Furthermore, the flexural strength of cement mortars with 0.05 wt.% GO and superplasticizer (SP) after 7 and 28 days increased by 12.26% and 21.86%, respectively, compared with reference mortar. At the same time, the effect of GO proved to be more significant and effective in the durability tests, suggesting that GO can enhance the microstructure through hydration products to create a highly cross-linked micro structure.

Keywords: Graphene oxide; Cement; Mechanical properties; Durability

1. Introduction

Nowadays, cementitious materials (CM) such as concrete and cement mortar are still the most widely used material in civil engineering and construction, being used for the construction of buildings, bridges, dams and tunnels [1], among others. The two main characteristics that define the quality of CM such as mortar are strength and durability. Strength is the ability of mortar to withstand loads (*e.g.*, compression and tension) and is influenced by a variety of factors, such as materials quality used, mixing method and curing process. Durability is the key factor in determining the service life of the CM, which can be defined as the mortar's ability to withstand chemical attacks (*e.g.*, CO_2 and Cl^-) and climatic conditions [2]. However, the main drawback that threatens CM is its inherent brittleness, which is due to its poor resistance to cracking, low tensile strength and high porosity, which can affect its mechanical properties and long-term durability [3,4]. In a bid to overcome the aforementioned drawbacks of CM, several studies advocate for the use of nanotechnology, which is considered one of the most reliable solutions due to the progress made and offers a tremendous opportunity to further improve the performance of CM as well as adjust its drawbacks by incorporating nanomaterials [5,6].

Nanomaterials are considered one of the most promising solutions due to their ability to reach the nanoscale level and affect the hydration products that are the main components determining the strength and durability of CM. The nanomaterials that have attracted the researchers' interest in the civil engineering field are numerous, being the most significant nano-silica (SiO_2) [7], nano-alumina (Al_2O_3) [8], carbon nanotubes (CNTs) [9] and, more recently, graphene oxide (GO) [10–19].

The graphene derivative, GO, exhibits extraordinary mechanical characteristics, including an intrinsic strength of around 130 GPa and a Young's modulus approximately 1 TPa [20]. However, has a high surface area and a unique structure, with various oxygen-containing functional groups situated at its basal plane and edge, such as hydroxyl (-OH), epoxide (C-O-C), carbonyl (C=O) and

 doi:10.20944/preprints202307.2114.v1

carboxyl (-COOH) [21]. The presence of these functional groups makes GO hydrophilic and therefore easily dispersible in water. For this reason, GO is considered one of the preferred nanomaterials to be incorporated into CM to form a homogeneous mixture that leads to better strength and durability [18,19,22,23].

Several papers have referred to the effects of GO modified cement-based materials, most of these investigations are focused on the mechanical strength and durability. Pan et al. [17] reported that the addition of 0.05% GO sheet into ordinary Portland cement paste increased the compressive and flexural strength by 15-33% and 41-58%, respectively. The reasons for the increase are probably due to the effect of GO on the hydration products, where chemical reactions among them produce strong interfacial forces, which could also be due to a strong interaction between GO sheets and cracks due to their 2D geometry. Gong et al. [16] found that the addition of 0.03% GO sheets to hardened cement paste rose the compressive strength by 46% and the tensile strength by almost 50%, owing to the enhancement of the hydration degree and the reduction of the porosity of the hardened cement paste. Furthermore, nuclear magnetic resonance (^{29}Si MAS-NMR) studies on tricalcium silicate (C_3S) conducted by Yang et al. [15] showed that adding GO to CM increases the hydration degree which obviously leads to an increase in compressive strength. Wang et al. [14] showed that 0.03% of GO caused a significant improvement in the mechanical properties of cement mortar after 28 days, compressive, flexural, and tensile strengths increased by 21.37%, 39.62, and 53.77% respectively.

As is also the case with durability, many studies have shown that the introduction of GO into CM results in varying degrees of improvement. Mohammad et al. [24] mentioned in their study that incorporating graphene oxide into a cement mortar makes it very resistant to chloride penetration due to the structure of the graphene oxide, which is intertwined and resembles a sponge structure that prevents the penetration of destructive particles such as chlorides ions. This can improve the durability of CM and increase the structures lifespan. According to the study of He et al. [25] GO effectively reduced the water absorption and gas permeability in cement mortar due to its application as a surface sealer.

With researching purpose of GO-modified cement mortar strengths and durability: first, a deep look at the nanoscale level is taken to reserach the effects of GO on cement paste such as hydration products and (C-S-H) gels chain structure, since are the mains contributors to the CM performance improvement, using TGA and ^{29}Si MAS-NMR characterization techniques. Subsequently, the effects of the of GO by different amount on the mechanical properties and durability of cement mortar were systematically studied, including compressive, flexural strengths, electrical resistivity, gas permeability and chloride diffusion. Cement mortar specimens were prepared with two different water/cement ratios: 0.5 and 0.35.

2. Materials and methods

2.1. Materials

To carry out the present research, cement mortars were prepared, in accordance with the EN 196-1 standard [26], mixing cement, sand, SP (only in the mix with ratio $w/c = 0.35$) and GO to evaluate the effect of the addition of this latter in the properties of pastes and mortars. For this purpose, Portland cement type CEM I 52.5R with high initial strength was used, whose composition is shown in Table 1. The GO commercial solution used was supplied from Graphenea with a concentration of 2 g/l. The elemental analysis of the GO is shown in Table 2. The commercial polycarboxylate-based superplasticizer (SP) was also used to ensure good dispersion of GO in mortars (only in mortars with w/c ratio 0.35). Lastly, CEN-NOMRSAND standardized sand was used for all mortars, according to the EN 196-1 standard [26], arranged in bags with 1350±5 g content.

Table 1. Chemical composition of Portland cement I 52.5 R.

CEM I	Chemical Composition (wt.%)							
	CaO	SiO_2	Al_2O_3	SO_3	Fe_2O_3	MgO	K_2O	LOI[1]
%	61.5	20.5	5.03	3.35	3.20	1.45	1.05	2.39

[1] Loss on ignition.

Table 2. Chemical composition of GO.

Element	Carbon	Hydrogen	Nitrogen	Sulfur	Oxygen
%	49-56	0-1	0-1	0-2	41-50

2.2. Preparation of GO-water suspension

The dispersion of GO in CM is critical because GO rapidly agglomerates within the cement matrix (especially as the w/c ratio was low) due to its high surface area and oxygen functional groups. Therefore, based on some researchers focused on this issue, it has been estimated that the best way to add GO to cement is to dissolve it in the mixing water firstly [13]. First, the amount of water required was weighed according to each dose, and then the volume of GO solution corresponding to the weight of the dose was pipetted into a pipette and then poured into the water weighed. After that, the GO-water suspension was stirred for 5 minutes with a magnetic stirrer at a rotation speed of 800 rpm. For samples prepared with SP, the SP was poured into GO-water suspension, stirring for another additional minute at the same speed of rotation. Figure 1.a depicts the GO dosages employed, as they appear different in staining, with the highest GO concentration being darker.

2.3. Preparation of mortar and paste samples

As previously mentioned, in this study two ratios *w/c* were chosen: 0.35 and 0.50 (with and without SP, respectively). The cement-to-sand ratio (*c/s*) was kept at 1/3, while three dosages of GO were used: 0.0005, 0.005 and 0.05% of the cement weight, as well as the fourth dose, was the reference one, without GO. Table 3 and Table 4 lists the mixed proportions of the GO-modified cement mortar prepared. The kneading procedure was prepared according to European standard EN 196-1:2018. The prepared GO-water suspension was placed in the mixing bowl along with the required cement powder, the mixing process was run at low speed for 30 seconds, then immediately switched to high speed as sand casting started for another 30 seconds, followed by a 90-second pause, after which the mixing process started again at high speed for 60 seconds.

In order to study the effect of GO on cement hydration process, GO-modified cement paste was prepared (*w/c* was kept 0.5 for all doses as indicated in the Table 3). The prepared GO-water suspension and the cement powder were placed in the mixing container, followed by kneading at low speed for 90 seconds. After 30 seconds of standing, the mixture was remixed for 90 seconds at low speed.

After the mixing process was completed, each fresh mixture was placed in a specific mold. The prepared mortar was placed in two types of molds. The first molds type was used to make prismatic specimens of dimensions 160x40x40mm^3 (for mechanical testing). The fresh mix was placed in two layers and each layer was compacted with 60 strokes using an automatic compactor. The second type of molds used for mortars were cylindrical ø75x150mm^3 (for durability testing), in which the fresh mixture was poured in two layers and vibrated on a vibrating table to ensure good compaction. In addition, the cement pastes were made in the form of prismatic bars of dimensions 60x10x10mm^3 and were compacted as in the case of the prismatic mortar specimens. Lastly, all molds were covered with plastic sheet and placed in a curing chamber with controlled ambient conditions (20±2°C/RH >95%). All samples were demolded after 24h and kept in the curing chamber at the same conditions until the test day.

Preprints (www.preprints.org) | NOT PEER-REVIEWED | Posted: 31 July 2023 doi:10.20944/preprints202307.2114.v1

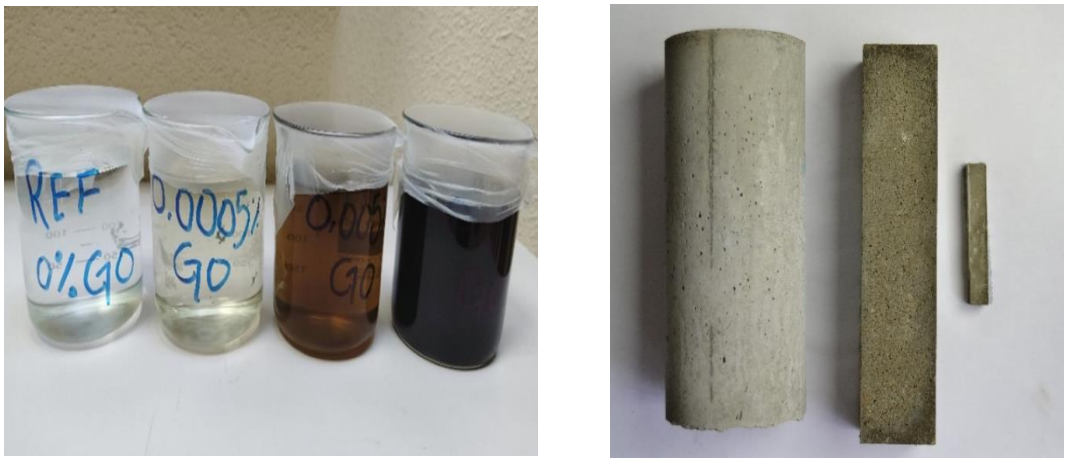

(**a**) (**b**)

Figure 1. (**a**) The prepared GO-water suspension; (**b**) Specimens type fabricated.

Table 3. Mix proportions of cement mortar.

Samples	Cement (g)	w/c	GO (wt.%)	SP (wt.%)	Total water content (ml)			Sand (g)
					Distilled water	GO dispersion (2g/l)	SP*	
MG0	450	0.5	0	-	225.0	0	-	1350
MG0005	450	0.5	0.0005	-	223.875	1.125	-	1350
MG005	450	0.5	0.005	-	213.75	11.25	-	1350
MG05	450	0.5	0.05	-	112.5	112.5	-	1350
MGS0	450	0.35	0	2.0	148.5	0	9.0	1350
MGS0005	450	0.35	0.0005	2.0	147.375	1.125	9.0	1350
MGS005	450	0.35	0.005	2.0	137.25	11.25	9.0	1350
MGS05	450	0.35	0.05	2.3	34.65	112.5	10.35	1350

* The amount of SP is a function of obtaining the same runoff in all mortars.

Table 4. Mix proportions of cement paste.

Samples	Cement (g)	W/C	GO (wt.%)	Total water content (ml)	
				Distilled water	GO dispersion (2g/l)
CG0	450	0.5	0	225	0
CG0005	450	0.5	0.0005	223.875	1.125
CG005	450	0.5	0.005	213.75	11.25
CG05	450	0.5	0.05	112.5	112.5

2.4. Characterization techniques

2.4.1. Thermal Gravimetric Analysis (TGA)

Four cement paste samples were analyzed by thermogravimetric analysis (TG/DTG). Before the analysis, the hydration process of cement paste should be halted at the age necessary to analyze the samples. To stop the hydration process, the cement paste was subjected to vacuum for 30 minutes, then submerged in isopropanol for 24 hours, followed by another 24 hours in an oven at 60 °C. Lastly, the samples were crushed into a powder and stored till analysis day. ATD/TG profiles were recorded according to the ASTM E 1131 standard [27] using Setaram Labsys Evo TGA_DTA equipment. A total of 50-100 mg of each type of paste was heated at 10 °C/min up to 1100 °C. The paste samples were used as representatives of the corresponding mortars to optimize the evaluation results.

Preprints (www.preprints.org) | NOT PEER-REVIEWED | Posted: 31 July 2023 doi:10.20944/preprints202307.2114.v1

2.4.2. ^{29}Si Magic Angle Spinning Nuclear Magnetic Resonance

^{29}Si MAS-NMR was performed on crushed cement paste samples CG0 and CG05 at 7 and 28 days using a Bruker Spectrometer model A400 with a resonant frequency of 79.5 MHz, spinning speed of 10 kHz and 4μs for pulse width. Chemical shifts of ^{29}Si were referenced to Tetramethylsilane (TMS) at 0 parts per million (ppm). The data were processed using the commercial NMR software MestRenova, and the curve generated was constrained by the Gauss-Lorentz function.

2.4.3. Strength measurements

The flexural and compressive strength tests of the mortars were carried out with prismatic samples 160x40x40mm^3 after 2, 7, 28 and 90 days, following the procedures specified in the standard EN 196-1: 2018 [26]. The tests were carried out with a three-point bonding machine for a flexural test (Ibertest C1B1400), shown at Figure 2.a, and a hydraulic machine (Ibertest model HIB 150) for compressive testing, as is shown in Figure 2.b. The average flexural strength was obtained after conducting a test of 3 samples for each type. The remaining two halves of each sample of flexural test were used to assess the compressive strength (average value of six specimens).

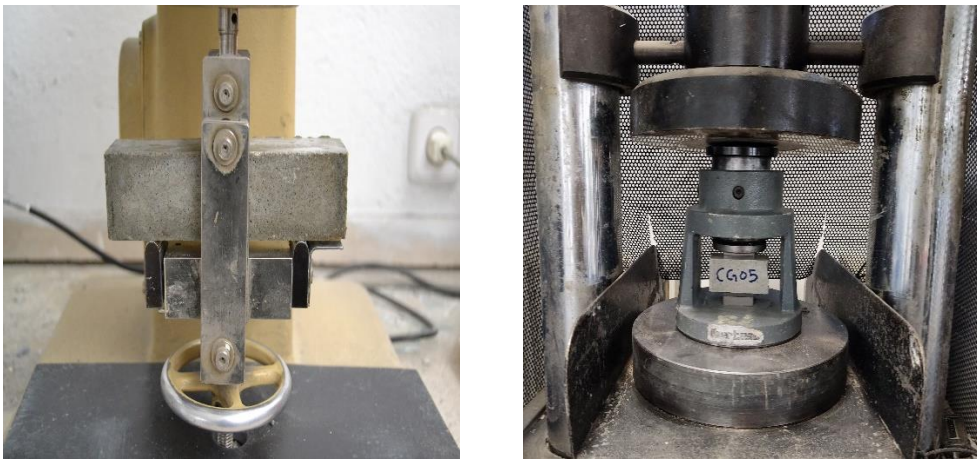

(**a**) (**b**)

Figure 2. Tests of (**a**) Flexural and; (**b**) compression strength.

2.4.4. Electrical resistivity

The two-electrode method was used by using Giatec RCON™ equipment to measure the electrical resistivity of 160x40x40 mm^3 prismatic mortar specimens at 2, 7, 28 and 90 days, in accordance with the Spanish standard UNE 83988-1:2008 [28]. The electrical resistivity was determined by using a two-pole that measured the electrical resistance to the passage of a certain current with frequencies that ranged between 1 Hz and 30 kHz, as shown in Figure 3. To calculate the electrical resistivity Equation (1) was used.

Preprints (www.preprints.org) | NOT PEER-REVIEWED | Posted: 31 July 2023 doi:10.20944/preprints202307.2114.v1

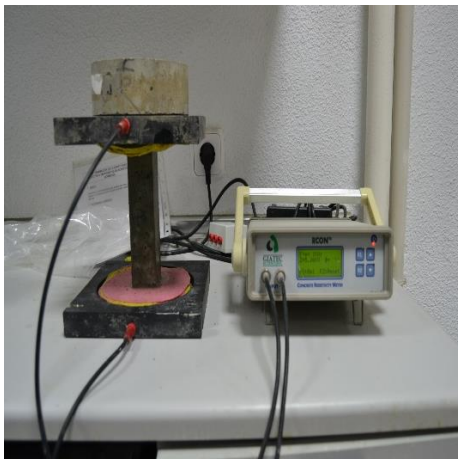

Figure 3. Electrical resistivity test.

$$R = V / I = \rho \times L/A \quad (1)$$

where, R is the electrical resistance, V is the difference potential, I is the current intensity, ρ is the electrical resistivity, L is the distance between the steel plates and A is the cross-sectional area of the specimen.

2.4.5. Oxygen permeability test

Oxygen permeability was determined on cylindrical mortar samples pieces ø75x50 mm^3, according to the UNE 83981:2008 standard [29] and RILEM-CEMBureau method [30]. After 28 days of curing in the curing chamber, samples were placed in a closed container with controlled environment (65%-75% relative humidity and 20±2°C temperature) for the purpose of drying of water droplets within the pores then achieving a steady weight. The method principle is to apply a specified pressure of oxygen gas to quantify the gas flow time through the sample. Equation (2) was used to calculate the oxygen permeability coefficient K for a given pressure P.

$$K\ (m^2) = \frac{2\ .\ Q\ .P_a\ .L\ .\ \eta}{A\ .(P^2 - P_a^2)} \quad (2)$$

where, Q is the volumetric flow rate, P_a is the atmospheric pressure, L is the specimen thickness, η is the dynamic oxygen viscosity, A is the section of the specimen and P is the applied pressure.

2.4.6. Chloride diffusion profiles

Chloride diffusion tests were performed according to Nordest NT Build 443 [31] to assess total chloride content. For the chloride penetration tests, cylindrical samples of ø75x150 mm^3 were used. After 28 days of curing in a humid chamber (98% relative humidity and 20±2°C temperature), the lower and lateral surfaces of each specimen were protected with an epoxy resin, leaving the upper circular face free to ensure that Cl^- diffusion occurred only through the upper face. The samples were then exposed for 35 days to water with sodium chloride (165±1g NaCl/1liter). After that period, different slices of each sample were extracted, obtained in the form of powder every mm of depth (8 slices of 1 mm each, up to 8 mm of depth were obtained) from the top. A suitable grinding wheel adapted to a drilling machine (Bosch Professional CGS 28 LCE) was used. Next, the extracted powder was dried at a temperature of 105 ± 5 °C for 24 h and, lastly, it was placed in a desiccator to prevent rehydration of the powder until the time of the test. The powder of these layers were then chemically analyzed for chloride concentration (total chloride) using a Metrohm model 916 Ti-Touch titrator.

Preprints (www.preprints.org) | NOT PEER-REVIEWED | Posted: 31 July 2023 doi:10.20944/preprints202307.2114.v1

3. Results and discussion

3.1. Effect of GO on the cement paste hydration process

The hydration process of four kinds of cement pastes (CG0, CG0005, CG005, and CG05) at 7 and 28 days was studied, As well as the hydration products amount of C-S-H and CH were assessed, to address the relationship between the hydration process and mechanical strength. The thermogravimetric analysis (TGA), as derivative thermogravimetric (DTG), was used to identify the detected phase. According to Figure 4, the DTG curves include three significant peaks. The first peak appearing in 105–430 °C due the loss of bound water due to the decomposition of calcium silicate hydrate C–S–H. The second peak corresponds to the dihydroxylation of calcium hydroxide CH that appear in 430–530 °C. And, the third peak located approximately at 550–1100 °C corresponds to the decarbonation of calcium carbonate $CaCO_3$ [32,33].

Figure 5 provides an overview of the cement paste weight losses at 7 and 28 days. The quantitative study of the first and second stages revealed that GO had no impact on the quantity of C-S-H and CH formed during cement hydration on the 7 days of curing. At 28 days of age, C-S-H amount increases with the increasing of GO dosage. The CG05 sample achieved the highest result, increasing by 5.46% in C-S-H compared with the reference sample CG0. In addition, GO does not have a significant effect on the CH amount produced even at advanced ages (28 days).

These results can be explained, that at the first moment, with the beginning of the hydration process, GO is considered as an absorbent of water, due to its large surface area and the active oxygen groups present in its layer. This absorption in water inhibits the hydration process in the early days, since causes a decrease in the water amount that the cement needs for reaction and therefore hydration, which results in a minority in the amount of C-S-H and CH produced in the early days. Nonetheless, over time, at 28 days, cement paste samples containing GO showed more C-S-H amount than the reference cement paste sample. The reason may be explained in this way: the hydration process can occur over the GO layer for a reason because it contains water, *i.e.*, attracting cement components, and forming hydration products on top of the GO layer, since it's well-known that GO act as a nucleation site [18]. As shown in the results, there has been an increase in the C-S-H at 28 days, while the study conducted by Li et al. [12] stated that the water absorbed in the early days is released, as a result, the C-S-H amount recovered in advanced ages. Previous research revealed similar outcomes to that presented in this work [34,35]. GO has a slight effect on stimulating the formation of more C-S-H amount, but the opposite with CH has no effect.

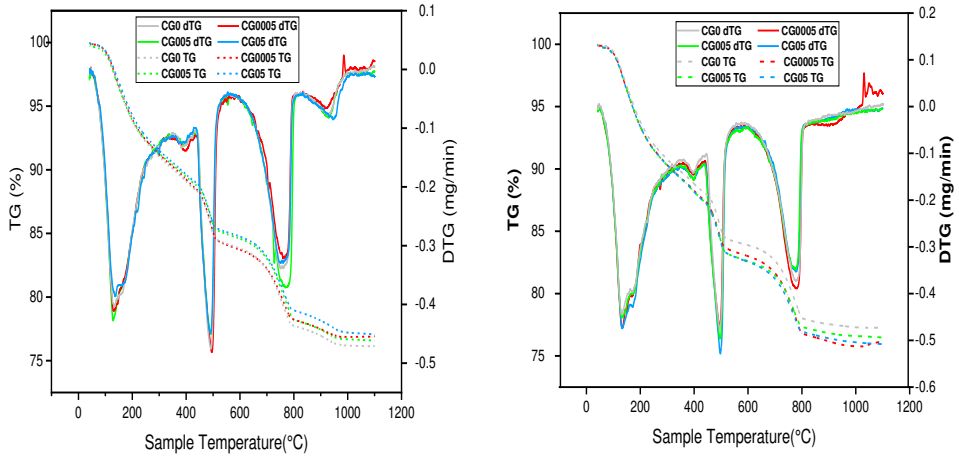

Figure 4. TGA and DTG curves of cement paste **a)** 7 days and **b)** days 28 days.

Preprints (www.preprints.org) | NOT PEER-REVIEWED | Posted: 31 July 2023 doi:10.20944/preprints202307.2114.v1

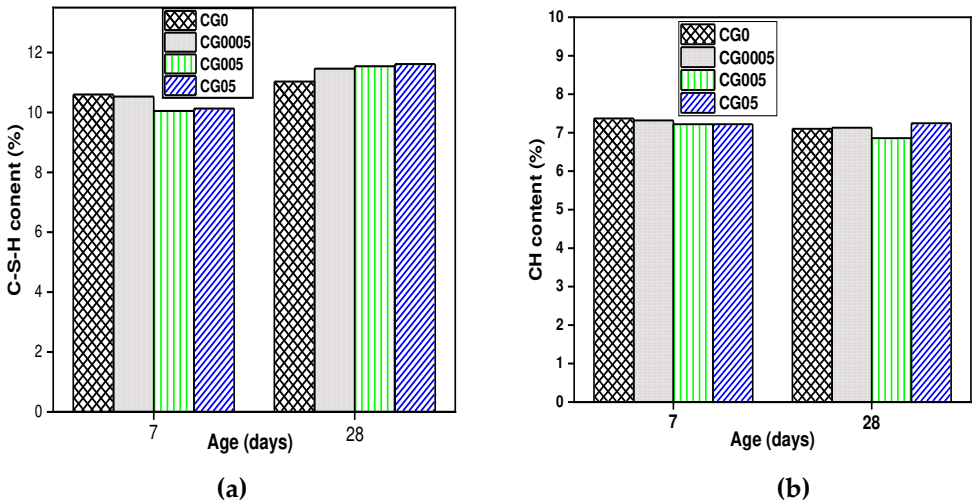

Figure 5. The hydration product content at 7 and 28 days: (a) C-S-H gel content and (b) CH Content.

3.2. ^{29}Si MAS-NMR characterization in pastes

The hydration degree and (C-S-H) gel structure of crushed cement pastes only on CG0 and CG05 were determined using ^{29}Si MAS-NMR spectroscopy after 7, and 28 days to gain a deeper insight into the formation phase (C-S-H) gel, which is the main hydration product contributing to the cohesion and strength of cementitious materials [33,36]. Furthermore, this allows for the observation of GO-induced changes in the C-S-H gel structure.

According to the findings of prior studies, Q^n species of silicate structures (n = 0-4), where Q denotes the silicate tetrahedron and n denotes the number of oxygen atoms interacting with nearby tetrahedrons. The shift around -68 to -74 ppm is associated to Q^0 which represents isolated tetrahedra. The shift located approximately at -76 to -80 ppm is linked to Q^1, represents beginning or end of silicate tetrahedra. As well Q^2 at -81.5 to -85.5 ppm approximately, represent the center site of the silicate chain, Q^2 may be further split into the bridging and pairing sites Q^{2b} and Q^{2p} respectively [37]. In this study, comparable results to previous studies were obtained [10,11].

As shown in Figure 6, the two samples CG0 and CG05 have similar absorption peaks Q^0, Q^1, Q^{2b} and Q^{2p} corresponding to the identical elements of the C–S–H gel constituents. However, the changing intensities highlight the variation in the chain structure. From data of Table 5, the mean chain length (MCL) and the hydration degree (α) of C–S–H were estimated using Equation (3) and Equation (4) respectively [10].

$$MCL = \frac{2 \times (Q^1 + Q^2)}{Q^1} \quad (3)$$

$$\alpha\ (\%) = \frac{(Q^1 + Q^2)}{(Q^0 + Q^1 + Q^2)} \times 100 \quad (4)$$

where, Q^n represent the integral intensities of the signals.

At 7 days the hydration degree together with the MCL of CG0 was higher than CG05. The reason may be due to the hydrophilic nature of GO, hence at the starting point of mixing it absorbs a certain amount of water and cement components, which disrupts the hydration process. Li et al. [12] also suggested that GO inhibits a certain way in the hydration process at early age due to its absorption of water, which leads to a decrease in the cement hydration degree.

At 28 days, the hydration degree and main chain length (MCL) of CG05 improved compared with CG0. The hydration degree of CG05 rose by 2.54% compared with CG0. As well, CG05 showed a greater MCL length of 7.01%, compared with CG0. The enhancement in the hydration degree and the main chain length can be attributed that the addition of GO can accelerate the hydration process

Preprints (www.preprints.org) | NOT PEER-REVIEWED | Posted: 31 July 2023 doi:10.20944/preprints202307.2114.v1

of cement at advanced ages, due to it effect as a nucleation site for the formation and development the hydrated products on it.

More detailed: first, the high surface area of GO serves as a deposition platform for the water and cement components that are adsorbed in the first days. As a result, the hydration degree increased. Second, the lengthening of the main chain MCL after addition of GO, could be due to the generation more tetrahedron Q^{2b}, as shown in Table 5, on the GO' surface area, since it is known that tetrahedron Q^{2b} be as bridge-shaped, therefore can act as point connection between short chains, generating a larger chain length. Similar results were found by Zhao et al. [11], reported that the effect of GO sheet as a nucleation site causes an increase in main chain length of C-S-H gels, resulting in an increased polymerization degree of C-S-H gels. It may be concluded that the nucleation site effect of GO accelerated the hydration process and increased the main chain length. These outcomes are consistent with what has been stated above in TGA results.

Table 5. Percentages of silicate chemical shift and parameters from deconvolution of ^{29}Si MAS-NMR spectra.

Sample	Q^0(%)	Q^1 (%)	Q^{2b} (%)	Q^{2p} (%)	α (%)	MCL
			7 days			
CG0	43.53	34.05	8.97	13.45	56.47	3.31
CG05	44.94	34.65	9.4	11.01	55.06	3.18
			28 days			
CG0	28.56	46.81	9.59	15.04	71.44	3.05
CG05	26.70	44.76	12.06	16.48	73.30	3.28

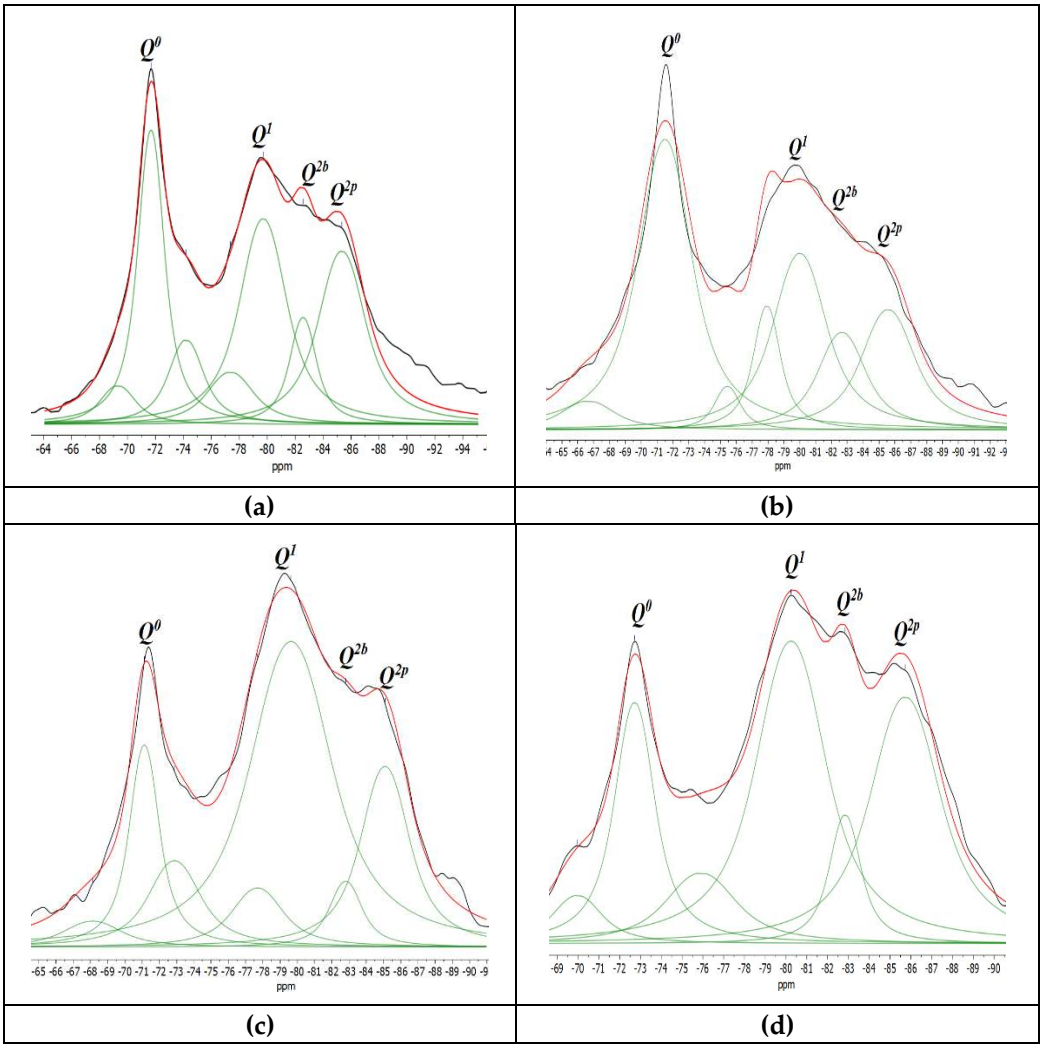

Preprints (www.preprints.org) | NOT PEER-REVIEWED | Posted: 31 July 2023 doi:10.20944/preprints202307.2114.v1

Figure 6. ^{29}Si MAS-NMR spectrums of (**a**) CG0 at 7 days; (**b**) CG05 at 7 days; (**c**) CG0 at 28 days; and (**d**) CG05 at 28 days.

3.3. Mechanical resistance in mortars

The effect of GO addition on the compressive and flexural strength of cement mortars, at different ages with two different water-cement ratios, is shown in Figure 7.

At 2 days, the addition of GO did not improve the compressive strength of either mortar (with or without SP). In addition, the results of flexural strength are similar in GO-modified cement mortar samples to the reference samples. As already mentioned in the TGA results, the C-S-H gels amount at first days, was low in GO-modified cement pastes compared with the reference sample. Since it is well-known that hydration products such as (C-S-H) gels are the main responsible for monitoring the mechanical strength of the cement composites.

At 7 days, the compressive strengths outcomes for both mortar (with and without SP) were not obvious yet. There were some improvements, but still slight, particularly in samples containing a small dosage of GO owing to the tiny quantity of water absorbed, since the bigger the dose, the more water absorbed, causing an inhibition of the hydration process. However, in contrast to compressive strength, both mortars improved in terms of flexural strength when compared with the reference sample. The samples manufactured just with GO (without SP), MG005 (0.005 wt.% GO), had the highest results, increasing by 5.63% compared with the control samples. The second mortar type (with SP), MGS05 showed the highest increment, rising by 13.98% compared with reference sample.s Might this be attributed to the cement matrix's good GO dispersion.

At 28 days, mechanical strength results, whether compressive or flexural, for all GO-modified cement mortar samples were greater than that of the reference sample. MG05 and MGS0005 had the biggest increase in compressive strength in comparison with the reference samples, increased by 9.33% and 8.45%, respectively. In terms of flexural strength, the two samples (with and without SP) that contain the highest GO dose obtained the maximum flexural strength, with MG05 rising by 19.72% and MGS05 by 30.85% in comparison with the reference samples. It is worth noting the effective role of SP in achieving good dispersion of GO.

Therefore, the GO effect as a nucleation site is the plausible explanation for GO's ability to contribute to mechanical strength enhancements for cement composites obtained at advanced ages. More precisely, at the beginning of the cement-water reaction, the added GO absorbs the components of water and cement, delaying the hydration process in the first days (there is already a hydration process, but only about GO), however, GO provides space as a platform for hydration products formed especially from water and cement components that has been absorbed. Most research that employed GO as a reinforcing agent provided an explanation for improving the mechanical strength of cement composites through the effect of GO as a nucleation site [13,38].

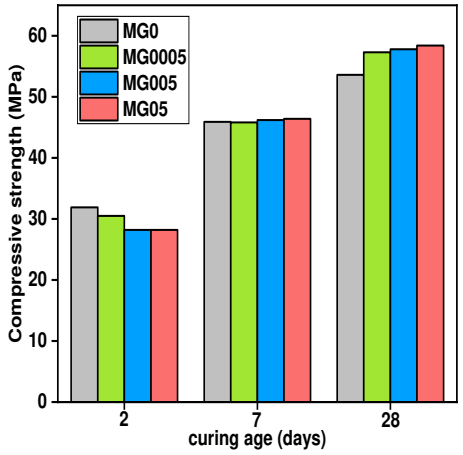

(**a**)

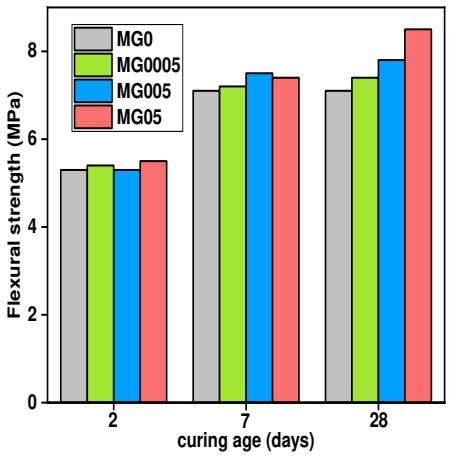

(**c**)

Preprints (www.preprints.org) | NOT PEER-REVIEWED | Posted: 31 July 2023 doi:10.20944/preprints202307.2114.v1

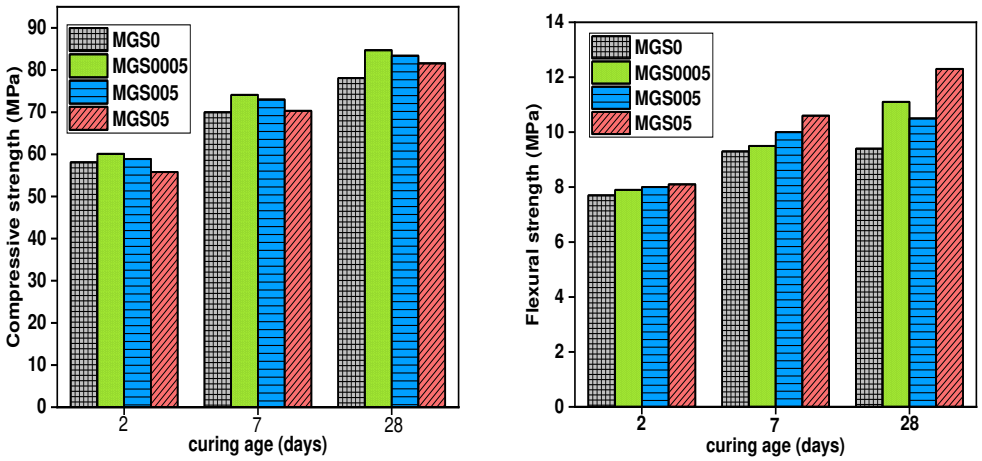

(b) **(d)**

Figure 7. Compressive strength average of mortar samples **a)** without SP **b)** with SP, and Flexural strength average of mortar samples **c)** without SP **d)** with SP.

3.4. Electrical resistivity in mortars

As shown in Figure 8, the results on electrical resistivity of the cement mortar samples was obtained (2, 7, 14, 28 days). The electrical resistivity gradually increases with the increase of curing age for all mortars. The reference sample's electrical resistivity (MGO) was determined to be 14.66, 28.75, 35.24 and 38.05 (Ω.m), as well MGS05, was found to be 37.06, 62.49, 72.97 and 83.22 (Ω.m) at curing ages of 2, 7, 14 and 28 days respectively. Until the 7th day, the electrical resistivity for all samples manufactured with GO for both types, with and without SP, was lower than that of the reference samples MGO. Therefore, as stated above in TGA and ^{29}Si MAS-NMR results, this may be because samples with the highest GO content absorb more water at first days, resulting in a reduction of C-S-H gels quantity formed. From 14 days, opposite outcomes were observed. All samples containing GO, both types (with and without SP) showed higher electrical resistivity than the reference sample. MG05 has the highest electrical resistivity tested compared with the MG0, the increase was 8.83% for 14 day curing and 21.37% for 28 day curing. For the second type of mortar, prepared with SP, the highest value of electrical resistivity was recorded for MGS05 sample, and the increases were 2.04% and 11.91% for 14 and 28 days of curing, respectively.

The electrical resistivity results were consistent with those of the previously mentioned TGA and ^{29}Si MAS-NMR. The higher electrical resistivity is explained by the production of more C-S-H gels at advanced ages (from 14 days), due to the nucleation effect of GO in the GO-modified cement samples, whereby hydration products such as (C-S-H) gels improve the cement matrix by plug pores, thus impeding the ionic conduction pathway. As, mentioned in these studies [19,39]. The improvement in electrical resistivity is attributed to the acceleration of the cement hydration process, which is caused by GO due to its acting as nucleation sites.

Preprints (www.preprints.org) | NOT PEER-REVIEWED | Posted: 31 July 2023 doi:10.20944/preprints202307.2114.v1

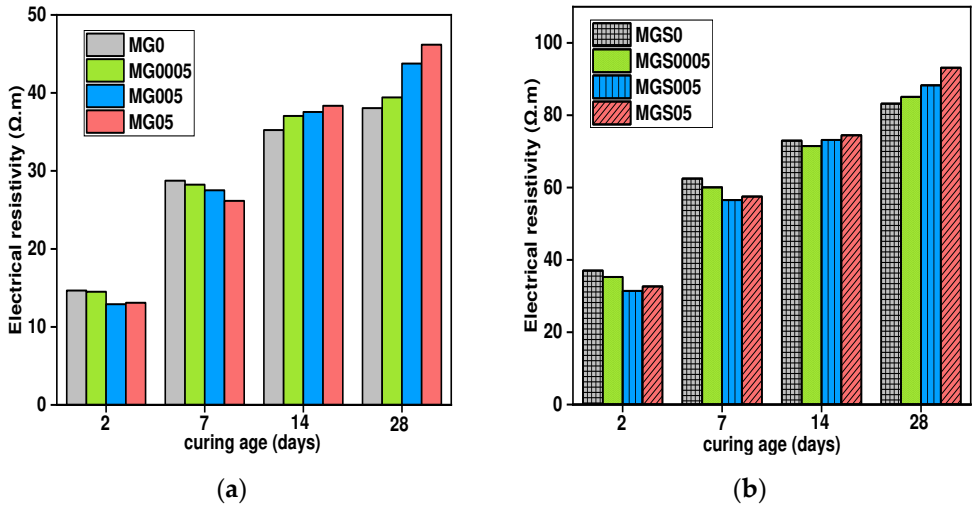

Figure 8. Electrical resistivity average of mortar samples **a)** without SP and **b)** with SP.

3.5. Gas permeability

The gas permeability coefficients of all mortar samples are shown in Figure 9. As can be seen, the gas permeability coefficient had significantly reduced for all cement mortars containing GO. Knowing that the variable was determined by testing three cylindrical pieces of mortar of each type. Compared with the control mortar, the gas permeability coefficients of MG0005, MG005 and MG05 decreased by 39.00%, 70.35 and 92.86%, respectively. As for the second type made with SP, MGS0005, MGS005 and MGS05 were reduced by 15.30%, 57.89% and 71.71%, respectively. The structure and volume of pores are one of the most significant aspects in microstructure that impacts the service-life of cementitious materials such as concrete, consequently, gas permeability is regarded as one of the approaches to extract information about the structure and volume of pores. The gas permeability results obtained were in good agreement with the results of the electrical resistivity test (Figure 8). As can be seen in Figure 9. GO-modified mortar samples had a very low gas permeability coefficient, indicating that the majority of the pores were clogged (i.e., their volume reduced, or their structure altered). It is well known that clogged pores impede the ionic conduction path, thus increase electrical resistivity. According to Wang *et al.* [40], the addition of GO reduces the pore volume with age, especially the macroscopic pores (larger than 50 nm) that contribute to the strength and permeability of the cement. Previous results demonstrates that GO accelerates the hydration process, due to its effect as a nucleation site. As indicated before, this impact increases the hydration products quantity, so intensifying the cement microstructure and causing a decrease and change in the volume and structure of pores. It is also feasible that the morphology of the hydration products precipitated on GO can be altered, that is, it becomes smaller, allowing them to fill the holes. Therefore, the morphology of the hydration product should be studied later.

Preprints (www.preprints.org) | NOT PEER-REVIEWED | Posted: 31 July 2023 doi:10.20944/preprints202307.2114.v1

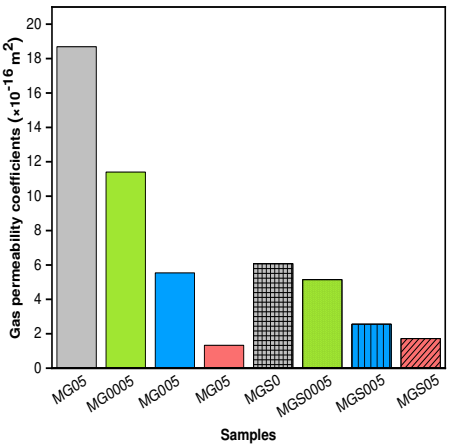

Figure 9. Gas permeability of mortars.

3.6. Chlorides diffusion in mortars

The coefficient of chloride diffusion is one of the most critical durability factors, since it is referred to chloride penetration into concrete and hence steel reinforcement corrosion. Figure 10 depicts the content of chloride ion vs. depth for cement mortar samples with varying amounts of GO. As observed from the curve, the chloride ion content of all cement mortar samples declines with increasing depth. Moreover, the total chloride content was greater at MG0, for all depths, except for the initial depth (MG0005 was the largest). Similarly, in the second type of mortar made with SP. Compared with reference sample MGS0, all GO-modified cement mortar samples showed a lower amount of chloride content at all depths. It should be noted also, that sample MGS0005 showed lower chloride content than sample MGS005 almost at all depths. While the MGS05 sample still had the best results in the sense of low chloride content at all depths.

In addition, in terms of comparing the two kinds of mortar, manufactured with or without SP: all samples manufactured with SP showed the best results, meaning less chloride content, than those manufactured without SP. This observation can be explained by the efficient function of SP in enhancing GO dispersion in the cement matrix. Consequently, the findings of this research demonstrated that the GO incorporation into cement mortar significantly increases its resistance to chloride ion penetration. This is consistent with past studies [23,41]. For the purpose of providing an explanation or a vision of the results obtained, it should be recalled that in the results of gas permeability, related to porosity, in the samples of modified cement mortar with GO, porosity decreased.

As well-known, the porosity is the main factor determining the cementitious materials service-life, *i.e.*, the likelihood of a chemical attacks (CO_2 or Cl^-, among others) on concrete increases with pore volume, and vice versa. As revealed in TGA and ^{29}Si MAS-NMR results, GO can accelerate the hydration process because it has the advantage of providing an adsorption site where more hydration products are formed. As a result, an increase in the amount of hydration products formed changes the microstructure of the cement mortar and forms a dense cross-linked structure, with a reduction in pore volume, further preventing chloride ions from entering the cement mortar. It is also possible to make a correlation with the results of the electrical resistivity test, because the higher electrical resistivity indicating a higher resistance to aggressive attack.

Preprints (www.preprints.org) | NOT PEER-REVIEWED | Posted: 31 July 2023 doi:10.20944/preprints202307.2114.v1

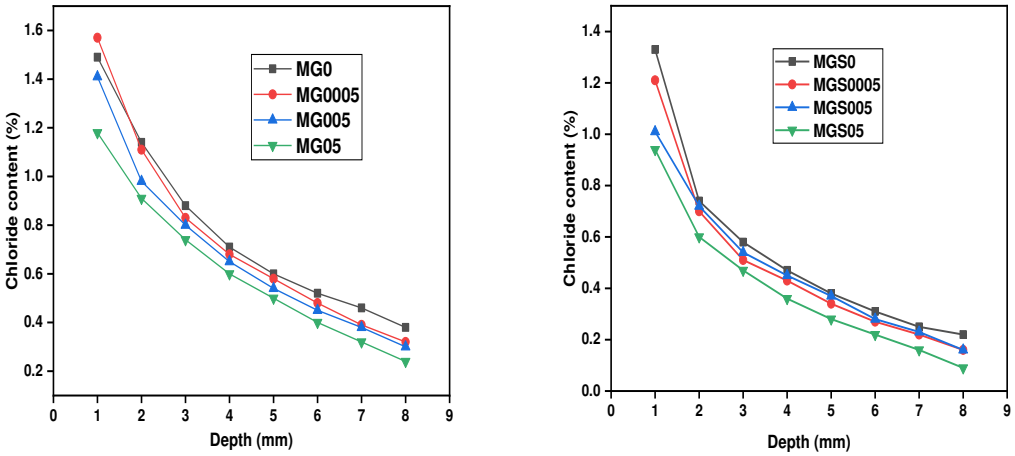

Figure 10. Total chloride ion content of cement mortars **a)** samples without SP and; **b)** samples with SP.

4. Conclusions

This research studied the effect of GO on the mechanical properties and durability of mortar. On the basis of the collected findings, the following conclusions may be drawn:

- According to the results of thermogravimetric analysis (TGA): at 7 days GO has no significant effects on the contents of both C-S-H and CH formed, while at 28 days the sample containing 0.05 wt.% GO showed the largest content of C-S-H, the increase was estimated by 5.46% compared with the reference sample, due to the fact that the GO acts as a nucleation site.
- The ^{29}Si MAS-NMR findings were comparable with the TGA results. The ^{29}Si MAS-NMR tests revealed that the addition of GO increased the hydration degree, along as enhanced in the main chain length value at 28 days.
- In mechanical strength results, GO was found to be more effective at advanced ages. With the addition of 0.05%, at 28 days, an increase in the flexural resistance of both types of mortar was observed, the flexural strength of MG05 increased by 19.72% and MG05 by 30.85%. It is worth noting the effective role of SP in achieving good dispersion of GO. In terms of compressive strength, GO-containing samples achieved slight improvements, MG05 increased by 9.33%, and MGS0005 by 8.45% compared with the reference samples. This improvement was due to a variety of GO-specific enhancement mechanisms, such as accelerated cement hydration process due to GO's impact as a nucleation site.
- In addition, it was found that the role of GO is more effective in durability tests. Increase in electrical resistivity and resistance to chloride ion penetration are directly proportional to a reduction in the gas permeability coefficient.

Author Contributions: Conceptualization, A.P., A.M. and J.C.G.; methodology, A.P., M.A.R., A.M. and J.C.G.; software, L.D. and A.P.; validation, L.D., A.P., M.A.R., A.M. and J.C.G.; formal analysis, M.G.A., J.C.G. and R.M.P. ; investigation, L.D., A.P., M.A.R., A.M. and J.C.G.; resources, A.M. and J.C.G..; data curation, L.D., A.P., M.A.R., A.M. and J.C.G.; writing—original draft preparation, L.D., A.P. and M.A.R.,; writing—review and editing, A.M. and J.C.G.; visualization, L.D., A.P., M.A.R., A.M. and J.C.G.; supervision, A.P., A.M. and J.C.G.; project administration, A.P., M.A.R., A.M. and J.C.G.; funding acquisition, A.M. and J.C.G.; All authors have read and agreed to the published version of the manuscript.

Funding: This research was funded by the Ministry of Science and Innovation of Spain through the Research Fund Project PID2019-108978RB-C31 and TED2021-130734B-I00.

Institutional Review Board Statement: Not applicable.

Informed Consent Statement: Not applicable.

Data Availability Statement: The data presented in this study are available on request from the corresponding author.

Conflicts of Interest: The authors declared no conflict of interest.

References

1. C.R. Gagg, Cement and concrete as an engineering material: An historic appraisal and case study analysis, Eng Fail Anal. 40 (2014) 114–140. https://doi.org/10.1016/j.engfailanal.2014.02.004.
2. M.A. Alam, M.Z. Habib, A. Hasan, R. Sheikh, A Study on the Quality Control of Concrete Production in Dhaka City Performance Evaluation of MS Tube Coupler on Axial Load Capacity of Column View project A Study on the Quality Control of Concrete Production in Dhaka City, IOSR Journal of Mechanical and Civil Engineering (IOSR-JMCE. 13 (n.d.) 89–98. https://doi.org/10.9790/1684-1303038998.
3. K.Y. Kim, T.S. Yun, K.P. Park, Evaluation of pore structures and cracking in cement paste exposed to elevated temperatures by X-ray computed tomography, Cem Concr Res. 50 (2013) 34–40. https://doi.org/10.1016/j.cemconres.2013.03.020.
4. K. van Tittelboom, N. de Belie, F. Lehmann, C.U. Grosse, Acoustic emission analysis for the quantification of autonomous crack healing in concrete, Constr Build Mater. 28 (2012) 333–341. https://doi.org/10.1016/j.conbuildmat.2011.08.079.
5. L. Raki, J. Beaudoin, R. Alizadeh, J. Makar, T. Sato, Cement and concrete nanoscience and nanotechnology, Materials. 3 (2010) 918–942. https://doi.org/10.3390/ma3020918.
6. L. Czarnecki, Sustainable concrete; is nanotechnology the future of concrete polymer composites?, in: Adv Mat Res, 2013: pp. 3–11. https://doi.org/10.4028/www.scientific.net/AMR.687.3.
7. L.P. Singh, S.R. Karade, S.K. Bhattacharyya, M.M. Yousuf, S. Ahalawat, Beneficial role of nanosilica in cement based materials - A review, Constr Build Mater. 47 (2013) 1069–1077. https://doi.org/10.1016/j.conbuildmat.2013.05.052.
8. Z. Li, H. Wang, S. He, Y. Lu, M. Wang, Investigations on the preparation and mechanical properties of the nano-alumina reinforced cement composite, Mater Lett. 60 (2006) 356–359. https://doi.org/10.1016/j.matlet.2005.08.061.
9. F. Gao, W. Tian, Z. Wang, F. Wang, Effect of diameter of multi-walled carbon nanotubes on mechanical properties and microstructure of the cement-based materials, Constr Build Mater. 260 (2020). https://doi.org/10.1016/j.conbuildmat.2020.120452.
10. X. Kang, X. Zhu, J. Qian, J. Liu, Y. Huang, Effect of graphene oxide (GO) on hydration of tricalcium silicate (C 3 S), Constr Build Mater. 203 (2019) 514–524. https://doi.org/10.1016/j.conbuildmat.2019.01.117.
11. L. Zhao, X. Guo, Y. Liu, Y. Zhao, Z. Chen, Y. Zhang, L. Guo, X. Shu, J. Liu, Hydration kinetics, pore structure, 3D network calcium silicate hydrate, and mechanical behavior of graphene oxide reinforced cement composites, Constr Build Mater. 190 (2018) 150–163. https://doi.org/10.1016/j.conbuildmat.2018.09.105.
12. X. Li, C. Li, Y. Liu, S.J. Chen, C.M. Wang, J.G. Sanjayan, W.H. Duan, Improvement of mechanical properties by incorporating graphene oxide into cement mortar, Mechanics of Advanced Materials and Structures. 25 (2018) 1313–1322. https://doi.org/10.1080/15376494.2016.1218226.
13. X. Li, Y.M. Liu, W.G. Li, C.Y. Li, J.G. Sanjayan, W.H. Duan, Z. Li, Effects of graphene oxide agglomerates on workability, hydration, microstructure and compressive strength of cement paste, Constr Build Mater. 145 (2017) 402–410. https://doi.org/10.1016/j.conbuildmat.2017.04.058.
14. Y. Wang, J. Yang, D. Ouyang, Effect of graphene oxide on mechanical properties of cement mortar and its strengthening mechanism, Materials. 12 (2019). https://doi.org/10.3390/ma12223753.
15. H. Yang, M. Monasterio, H. Cui, N. Han, Experimental study of the effects of graphene oxide on microstructure and properties of cement paste composite, Compos Part A Appl Sci Manuf. 102 (2017) 263–272. https://doi.org/10.1016/j.compositesa.2017.07.022.
16. K. Gong, Z. Pan, A.H. Korayem, L. Qiu, D. Li, F. Collins, C.M. Wang, W.H. Duan, Reinforcing Effects of Graphene Oxide on Portland Cement Paste, Journal of Materials in Civil Engineering. 27 (2015). https://doi.org/10.1061/(asce)mt.1943-5533.0001125.
17. Z. Pan, L. He, L. Qiu, A.H. Korayem, G. Li, J.W. Zhu, F. Collins, D. Li, W.H. Duan, M.C. Wang, Mechanical properties and microstructure of a graphene oxide-cement composite, Cem Concr Compos. 58 (2015) 140–147. https://doi.org/10.1016/j.cemconcomp.2015.02.001.
18. M.M. Mokhtar, S.A. Abo-El-Enein, M.Y. Hassaan, M.S. Morsy, M.H. Khalil, Mechanical performance, pore structure and micro-structural characteristics of graphene oxide nano platelets reinforced cement, Constr Build Mater. 138 (2017) 333–339. https://doi.org/10.1016/j.conbuildmat.2017.02.021.
19. W. Li, X. Li, S.J. Chen, Y.M. Liu, W.H. Duan, S.P. Shah, Effects of graphene oxide on early-age hydration and electrical resistivity of Portland cement paste, Constr Build Mater. 136 (2017) 506–514. https://doi.org/10.1016/j.conbuildmat.2017.01.066.
20. L. Liu, J. Zhang, J. Zhao, F. Liu, Mechanical properties of graphene oxides, Nanoscale. 4 (2012) 5910–5916. https://doi.org/10.1039/c2nr31164j.
21. B. Gupta, N. Kumar, K. Panda, V. Kanan, S. Joshi, I. Visoly-Fisher, Role of oxygen functional groups in reduced graphene oxide for lubrication, Sci Rep. 7 (2017). https://doi.org/10.1038/srep45030.

22. T.S. Qureshi, D.K. Panesar, Impact of graphene oxide and highly reduced graphene oxide on cement based composites, Constr Build Mater. 206 (2019) 71–83. https://doi.org/10.1016/j.conbuildmat.2019.01.176.
23. A. Mohammed, J.G. Sanjayan, W.H. Duan, A. Nazari, Incorporating graphene oxide in cement composites: A study of transport properties, Constr Build Mater. 84 (2015) 341–347. https://doi.org/10.1016/j.conbuildmat.2015.01.083.
24. A. Mohammed, J.G. Sanjayan, W.H. Duan, A. Nazari, Graphene Oxide Impact on Hardened Cement Expressed in Enhanced Freeze–Thaw Resistance, Journal of Materials in Civil Engineering. 28 (2016). https://doi.org/10.1061/(asce)mt.1943-5533.0001586.
25. J. He, S. Du, Z. Yang, X. Shi, Laboratory investigation of graphene oxide suspension as a surface sealer for cementitious mortars, Constr Build Mater. 162 (2018) 65–79. https://doi.org/10.1016/j.conbuildmat.2017.12.022.
26. 27-000196NENN121_ES, (n.d.).
27. Standard Test Method for Compositional Analysis by Thermogravimetry 1, n.d. www.astm.org,.
28. UNE 83988–1, Concrete durability. Test methods. Determination of the electrical resistivity, 2008.
29. UNE 83981, Concrete Durability. Test Methods. Determination to gas permeability of hardened concrete, 2008. www.aenor.es.
30. J.J. Kollek, The determination of the permeability of concrete to oxygen by the Cembureau method-a recommendation, 1989.
31. Concrete, Hardened: Accelerated Chloride Penetration, (n.d.). www.nordtest.org.
32. W.J. Long, T.H. Ye, Y.C. Gu, H.D. Li, F. Xing, Inhibited effect of graphene oxide on calcium leaching of cement pastes, Constr Build Mater. 202 (2019) 177–188. https://doi.org/10.1016/j.conbuildmat.2018.12.194.
33. H.F.W. (Harry F.W.) Taylor, Cement chemistry, T. Telford, 1997.
34. Y. Wang, J. Yang, D. Ouyang, Effect of graphene oxide on mechanical properties of cement mortar and its strengthening mechanism, Materials. 12 (2019). https://doi.org/10.3390/ma12223753.
35. Q. Wang, S. Li, J. Wang, S. Pan, C. Lv, X. Cui, Z. Guo, Effect of Graphene Oxide on Hydration Process and Main Hydration Products of Cement, Kuei Suan Jen Hsueh Pao/Journal of the Chinese Ceramic Society. 46 (2018) 163–172. https://doi.org/10.14062/j.issn.0454-5648.2018.02.10.
36. I.G. Richardson, The calcium silicate hydrates, Cem Concr Res. 38 (2008) 137–158. https://doi.org/10.1016/j.cemconres.2007.11.005.
37. I. Kiur, B. Pollet, J. Virlet, A. Nonat, C-S-H Structure Evolution with Calcium Content by Multinuclear NMR, n.d.
38. F. Babak, H. Abolfazl, R. Alimorad, G. Parviz, Preparation and mechanical properties of graphene oxide: Cement nanocomposites, The Scientific World Journal. 2014 (2014). https://doi.org/10.1155/2014/276323.
39. R. Kaur, N.C. Kothiyal, Comparative effects of sterically stabilized functionalized carbon nanotubes and graphene oxide as reinforcing agent on physico-mechanical properties and electrical resistivity of cement nanocomposites, Constr Build Mater. 202 (2019) 121–138. https://doi.org/10.1016/j.conbuildmat.2018.12.220.
40. Q. Wang, J. Wang, C.X. Lu, B.W. Liu, K. Zhang, C.Z. Li, Influence of graphene oxide additions on the microstructure and mechanical strength of cement, Xinxing Tan Cailiao/New Carbon Materials. 30 (2015) 349–356. https://doi.org/10.1016/s1872-5805(15)60194-9.
41. S. Liu, F. Lu, Y. Chen, B. Dong, H. Du, X. Li, Efficient Use of Graphene Oxide in Layered Cement Mortar, Materials. 15 (2022). https://doi.org/10.3390/ma15062181.